

Effects of the Injection Inhomogeneity on the Detonation Propagation Speed in a Reflective Shuttling Detonation Engine Using Gaseous Fuel and Oxidizer

Ryuki Sato, Haruna Inoue, Akira Kawasaki
Shizuoka University
Hamamatsu, Shizuoka, Japan

Ken Matsuoka, Tasuku Nagaoka, Yusuke Oda, Noboru Itouyama, Jiro Kasahara
Nagoya University
Nagoya, Aichi, Japan

Akiko Matsuo
Keio University
Yokohama, Kanagawa, Japan

1 Introduction

In detonation combustion, the total pressure of the burned gas increases due to fluid compression caused by the shock front in the detonation wave. Therefore, incorporating detonation into combustion devices can lead to an increase in the total pressure of the exhaust flow within the combustor [1]. This increase, commonly referred to as pressure gain, reduces the compression work required by pumps or compressors upstream of the combustor. As a result, it alleviates performance demands on the pressurization system and contributes to simplifying the overall system architecture.

However, the theoretical pressure gain has not yet been experimentally validated in continuously operating detonation engines, such as rotating detonation engines (RDEs) [2]. This discrepancy is primarily attributed to non-idealities in real detonation waves, such as secondary combustion and secondary shock waves [3]. These arise from inherent characteristics of actual flow and combustion fields, including incomplete mixing of fuel and oxidizer, interactions between burned and unburned gases, and injection inhomogeneity.

This study focuses specifically on the inhomogeneous injection of fuel and oxidizer. Injection inhomogeneity is an intrinsic non-ideality in continuously operating detonation engines, arising from the sparse introduction of unburned gas—supplied through injector orifices—into the burned gas region ahead of the detonation wave. Wang *et al.* [4] investigated detonation wave propagation through periodically inhomogeneous mixtures using two-dimensional numerical simulations. Their results

indicated that as the spatial scale of the inhomogeneity increases, the detonation cell width expands and the propagation speed decreases, eventually leading to detonation failure.

The objective of this study is to experimentally investigate the behavior of detonation waves propagating through a periodically inhomogeneous mixture and to assess the influence of injection inhomogeneity on detonation propagation speed.

2 Experimental Setup

The reflective shuttling detonation engine (RSDE) used in this study is a type of continuously operating detonation engine designed to enable optical visualization of propagating detonation waves within the combustor. As illustrated in Figure 1, the combustor has a length (L) of 36 mm in the flow direction (Z -axis), a width (W) of 90 mm perpendicular to the flow (X -axis), and a depth (D) of 5 mm along the line of sight (Y -axis).

Detonation waves are initiated by a pre-detonator and propagate in the width-wise direction of the combustor, reflecting off the side walls in a shuttling manner. The continuous propagation of the detonation wave is sustained by the injection of unburned gases through a series of injector orifices. The flow and combustion characteristics in the RSDE share several similarities with those observed in RDEs.

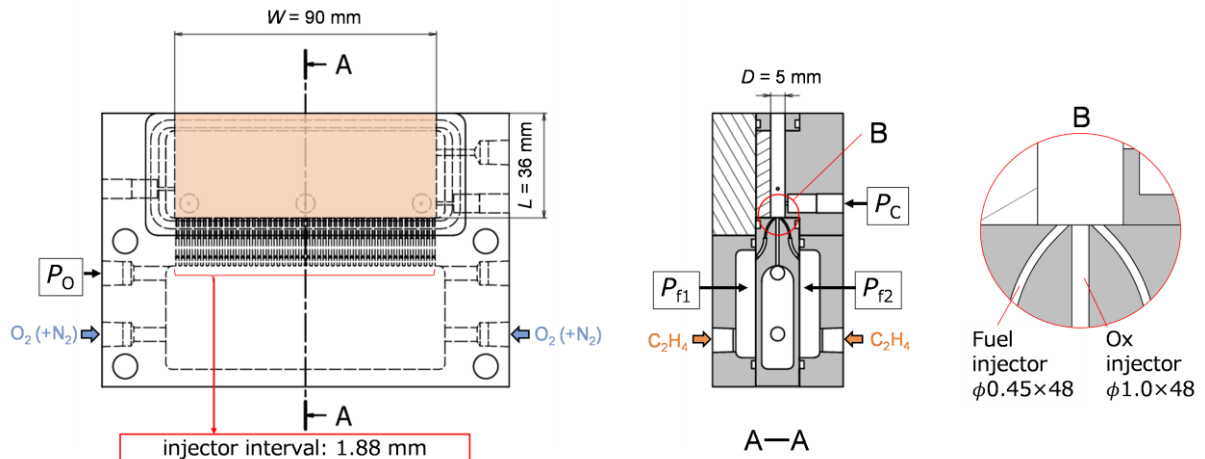


Figure 1: Schematic of the test rig (RSDE). Measurement points of pressure are indicated.

Table 1: Summary of the experimental conditions and results.

Run #	P_{f1} kPa	P_{ox} kPa	P_b kPa	\dot{m}_f g/s	\dot{m}_{ox} g/s	ϕ -	\dot{m}_{dil} g/s	X_{dil} %	P_{c1} kPa	N_w -
17	132	143	53.0	4.53	13.5	1.15	-	-	70.3	2
18	173	170	19.6	5.92	16.0	1.27	-	-	66.3	1
22	173	191	18.9	5.94	16.6	1.22	1.36	8.6	71.8	1
23	171	197	19.8	5.86	16.8	1.20	1.79	10.8	68.7	1
24	171	192	18.9	5.84	16.4	1.22	1.68	10.5	69.7	1
27	171	217	19.8	5.85	17.8	1.12	2.58	14.2	72.1	1

Table 1 summarizes the experimental conditions and results, including the fuel and oxidizer manifold pressures (P_{f1} and P_{ox}), buck pressure (P_b), fuel and oxygen flow rates (\dot{m}_f and \dot{m}_{ox}), equivalence ratio

(ϕ), diluent flow rate (\dot{m}_{dil}) and its mole fraction (X_{dil}) in the oxidizer, combustion pressure (P_{c1}), and the number of waves (N_{w}). The fuel used was C_2H_4 , the oxidizer was O_2 , and the diluent was N_2 . The diluent was introduced into the oxidizer supply line via a Tee-union to dilute the oxidizer.

Pressures were measured using pressure transducers (PAA-23SY, KELLER), and the diluent mass flow rate was measured using a mass flow meter (MQ-3000SLPM-D, ALICAT). The combustion pressure was measured at the center of the combustor wall in the width-wise direction. All pressure and flow rate values were averaged over the time interval from 500 to 550 ms after ignition, during which the conditions remained nearly steady, as will be described below.

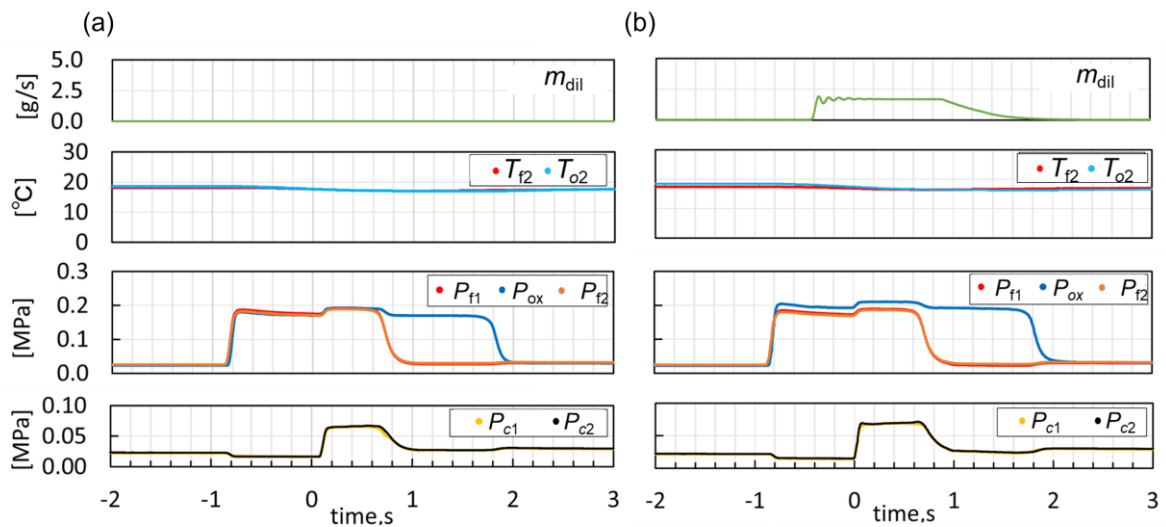


Figure 2: Typical time histories of measured data: temperatures (T_{f2} and T_{o2}) and pressures (P_{f1} , P_{f2} , and P_{ox}) within the fuel and oxidizer manifold, diluent flow rate (\dot{m}_{dil}), and combustor pressure (P_{c1} and P_{c2}). (a) Without dilution (Run #18). (b) With dilution (Run #24).

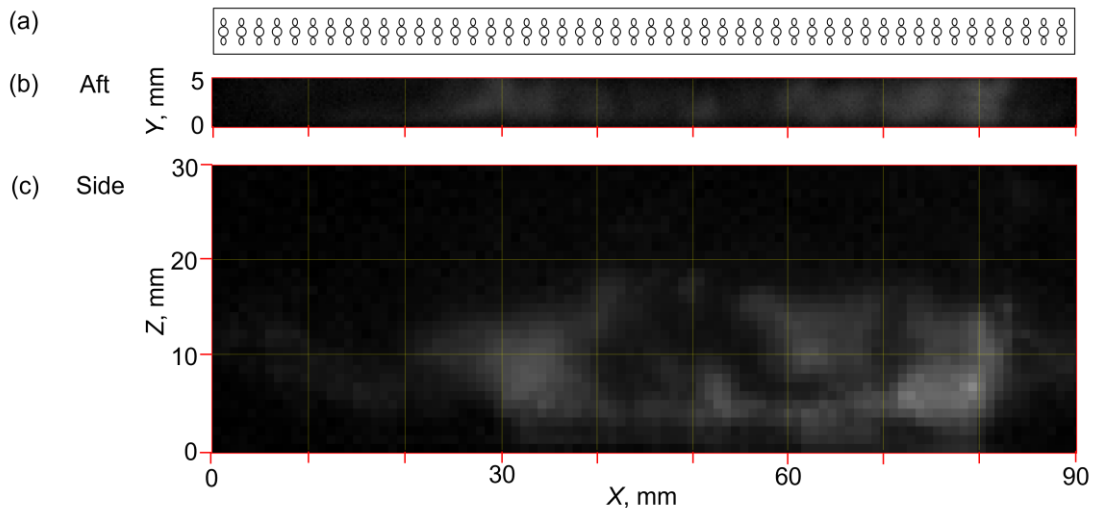


Figure 3: Typical chemiluminescence visualization results (Run #17, w/o dilution, $t = 400$ ms). (a) Injector pattern. (b) Aft view (0.27 mm/pixel). (c) Side view (0.88 mm/pixel).

3 Results and Discussion

Figure 2 presents typical time histories of the measured data. The ignition timing is defined as time zero on the horizontal axis. Steady operation was observed between 200 ms and 600 ms. Figure 3 shows representative chemiluminescence images of the combustor taken at 400 ms after ignition.

Figure 4(a) shows wave diagrams representing the temporal evolution of chemiluminescence distributions within the combustor from 500 to 501 ms after ignition. These diagrams were generated by stacking pixel lines in the X-direction at different Y-positions from aft-view chemiluminescence images along the time axis. Figure 4(b) presents the correlation coefficients of the wave diagrams with that at $Y = 2.5$ mm. The comparison indicates that there is no significant variation in wave behavior along the Y-direction.

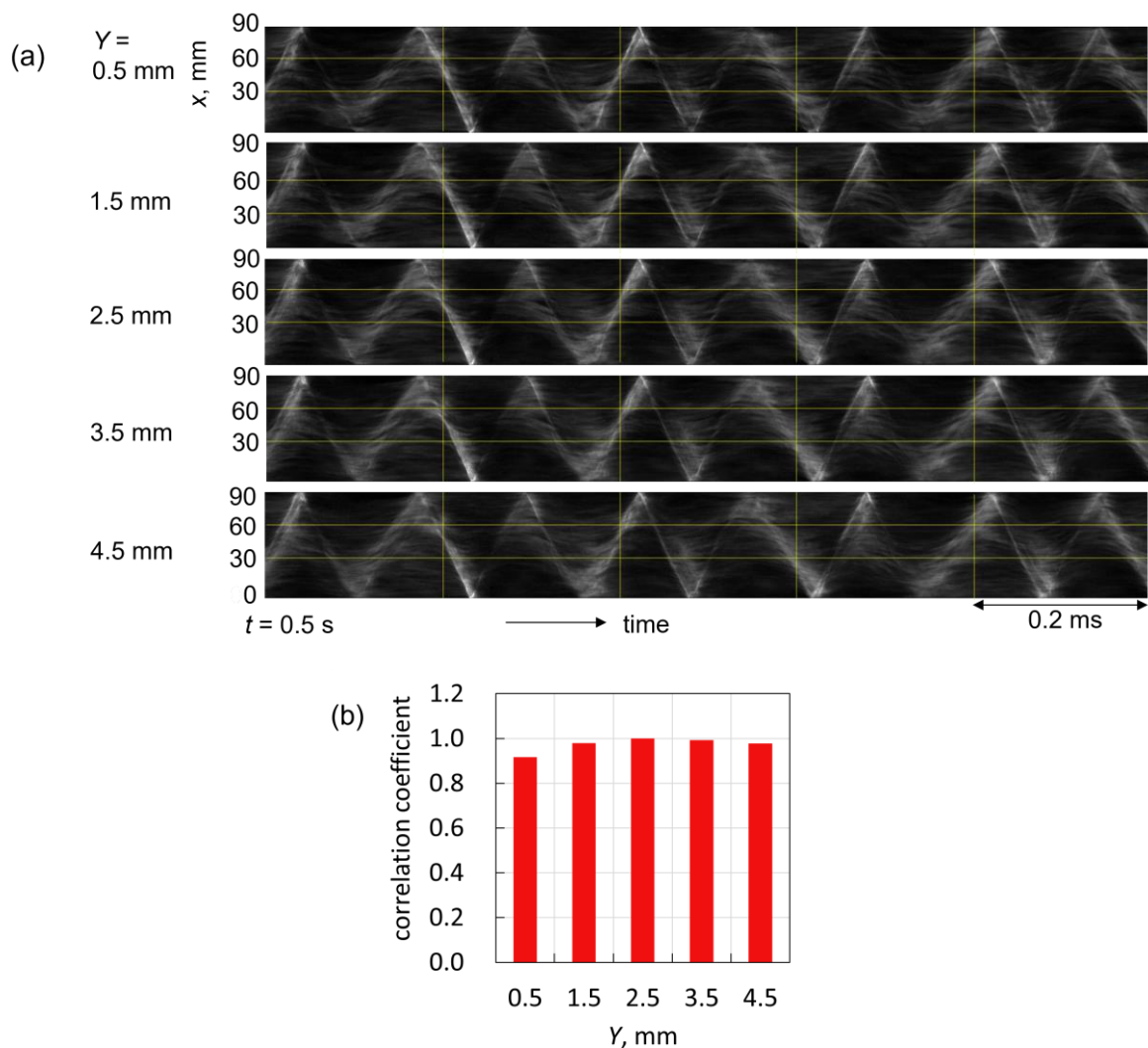


Figure 4: Comparison of wave propagation for different Y positions. (a) Wave diagrams made from chemiluminescence images for different Y positions (dilution ratio 10.5 %, Run #24) ($t = 500$ to 501 ms). (b) Correlation coefficients of the wave diagrams with the one at $Y = 2.5$ mm.

Figure 5 shows wave diagrams for dilution ratios of 0%, 10.5%, and 14.2%. Based on the confirmed uniformity in the Y -direction, the evaluation was conducted at the center along the Y -axis. Several distinct propagation patterns were observed, including single sharp waves, double co-propagating waves, crossing waves, and ambiguous waves, as shown in the figure. It can be observed that as the dilution ratio increases, the propagation speed decreases. Moreover, the local propagation velocity varies depending on the observed propagation mode.

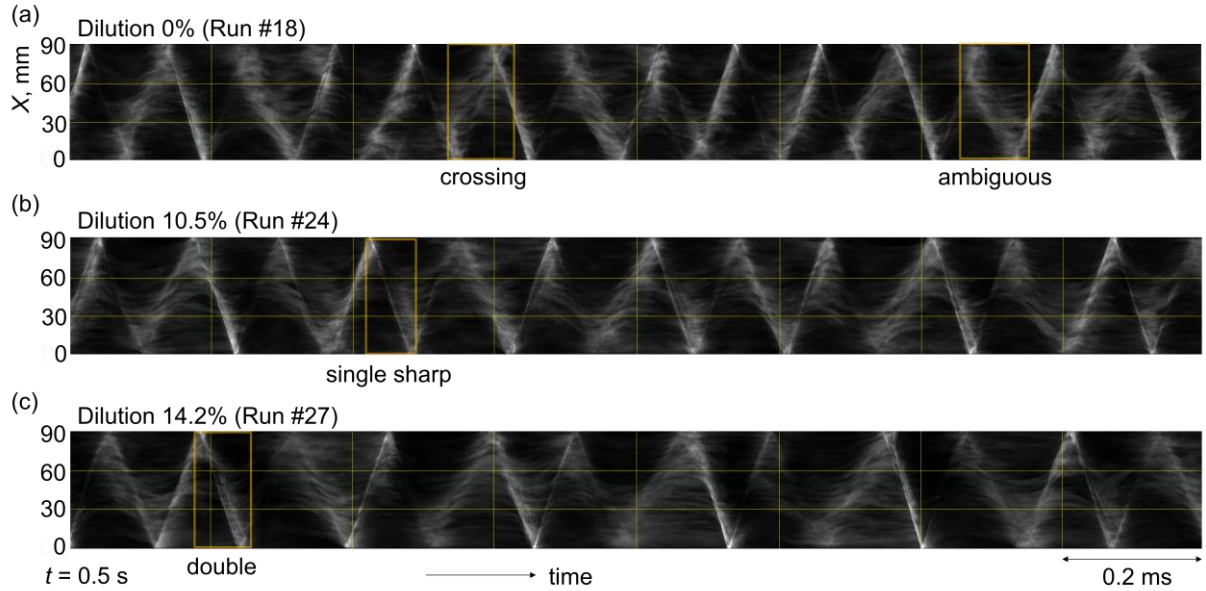


Figure 5: Wave diagrams from 500 to 516 ms from ignition for (a) 0% dilution (Run #18), (b) 10.5% dilution (Run #24), and (c) 14.2% dilution (Run #27). Spatial resolution = 1 mm and temporal resolution = 1 μ s.

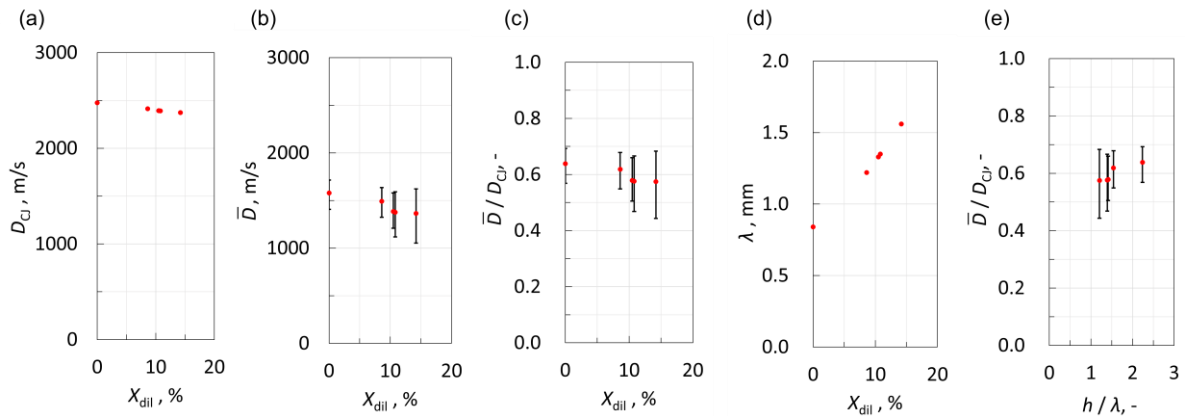


Figure 6: Effects of the dilution ratio (X_{dil}). (a) CJ velocity (D_{CJ}). (b) Average detonation velocity (\bar{D}). The velocity values were averaged over 20 shuttling cycles, and the error bars denote the range between the maximum and minimum velocities observed in those cycles. (c) Average detonation velocity normalized with CJ velocity (\bar{D}/D_{CJ}). (d) Cell width (λ). (e) Normalized detonation velocity vs non-dimensional injection interval (= injection interval / cell width, h/λ). Injection interval h is 1.88 mm.

Figure 6 shows effects of dilution ratio. In Figs. 6(a) and 6(b), as the dilution ratio increases, both the CJ velocity D_{CJ} and the average detonation velocity \bar{D} tend to decrease. Figure 6(c) shows that as the dilution ratio increases, normalized velocity (Average velocity / CJ velocity, \bar{D}/D_{CJ}) tends to decrease as well. Figure 6(d) shows that as the dilution ratio increase, the cell width increases. Figure 6(e) shows that as non-dimensional injection interval (= injection interval / cell widths, h/λ) increase, normalized velocity tends to increase.

4 Conclusions

In this study, an RSDE operating with gaseous ethylene as fuel and gaseous oxygen as oxidizer was investigated. Chemiluminescence within the combustor was visualized from both the aft end and the side, with spatial and temporal resolutions of approximately 1 mm and 1 μ s, respectively. To examine the effects of injection inhomogeneity on the propagation velocity of detonation waves, the non-dimensional injection interval—defined as the ratio of the injector spacing h to the detonation cell width λ —was varied by diluting the oxidizer with gaseous nitrogen. Based on the results, the following conclusions can be drawn:

- Under the conditions examined in this study, the normalized propagation velocity of the detonation wave increased with the non-dimensional injection interval.
- Multiple propagation patterns were observed during steady operation, and the propagation velocity varied depending on the specific propagation pattern.

Acknowledgements

This work was partially supported by JSPS KAKENHI Grant Numbers JP22K14422, JP23KK0082, and JP23K20036.

References

- [1] Gutmark EJ. (2021). Pressure gain combustion. *Shock Waves*. 31: 619.
- [2] Yamaguchi M, Matsuoka K, Kawasaki A, Kasahara J, Watanabe H, Matsuo A. (2019). Supersonic combustion induced by reflective shuttling shock wave in fan-shaped two-dimensional combustor. *Proc. Combust. Inst.* 37: 3741.
- [3] Raman V, Prakash S, Gamba M. (2023). Nonidealities in Rotating Detonation Engines. *Annu. Rev. Fluid Mech.* 55: 639.
- [4] Wang Y, Huang C, Deiterding R, Chen H, Chen Z. (2023). Numerical studies on detonation propagation in inhomogeneous mixtures with periodic reactant concentration gradient. *J. Fluid Mech.* 955: A23.